Available online at www.sciencedirect.com
SCIENCE DIRECT®
Journal of Nuclear Materials 337–339 (2005) 1–9
journal of nuclear materials
www.elsevier.com/locate/jnucmat

Material migration in divertor tokamaks

G.F. Matthews *

JET Joint Undertaking, UKAEA/Euratom Fusion Association, Culham Science Centre, Abingdon, Oxfordshire, Oxon OX14 3DB/3EA, UK

Abstract

Erosion of plasma facing material, its transport through the plasma and its deposition define the topic of material migration. It is a subject which is a pivotal issue both for ITER and for the longer term economic and technological viability of fusion power. This review summarises the current status and future direction of this field.

PACS: 52.55.Fa; 52.40.
Keywords: Erosion and deposition; First wall; Fusion reactor

1. Introduction

The topic of impurity migration in divertor tokamaks covers all processes leading to erosion, transport and re-deposition of impurities. This paper presents a review and long term outlook.

Poloidal divertors [1] have been very successful at localising the interactions of plasma ions with the target plate material in a part of the machine geometrically distant from the main plasma where any impurities released are well screened from the main plasma and return to the target plate [2]. Atoms sputtered from the target plate become ionised, Fig. 1, and are transported through the plasma primarily under the influence of the ion temperature gradient force which drives impurities out of the divertor and friction with the flow of deuterium into the divertor which returns them to the plate [3]. Other lesser forces include the electron temperature gradient force and electric field [2]. Since the divertor is the place where ion and neutral fluxes are highest and screening of impurities from the main plasma is good, a local view of divertor target lifetime is quite common in the literature and is embodied in Monte-Carlo impurity transport codes like ERO [4] and RE-DEP [5] which treat impurity migration within a single divertor leg as essentially an isolated system. In this picture, target material is eroded from the near the strike point by physical and chemical sputtering and deposited in the private region or outer SOL. Target lifetime is then simply viewed as the time taken to erode through the tile to the coolant channel or heat-sink material beneath. Tritium retention in the re-deposited material also presents challenges for future devices since safety considerations place strict limits on the total amount of tritium retained in the vessel [6].

The simple picture of local erosion and re-deposition within an isolated divertor leg can be a reasonable approximation to reality in the outer divertor when limited numbers of attached plasmas are analysed. An example of this is given in Fig. 2 [7] where erosion/deposition of amorphous carbon-hydrogen films (a-C:H) was measured in situ pulse to pulse for short (1s) hot ion

* Tel.: +44 1235 464523; fax: +44 1235 464766.
E-mail address: gfm@jet.uk

0022-3115/$ - see front matter
doi:10.1016/j.jnucmat.2004.10.075

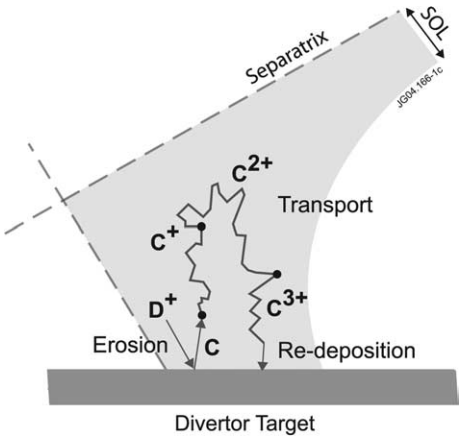

Fig. 1. Local view of the cycle of erosion re-deposition within a leg of the divertor.

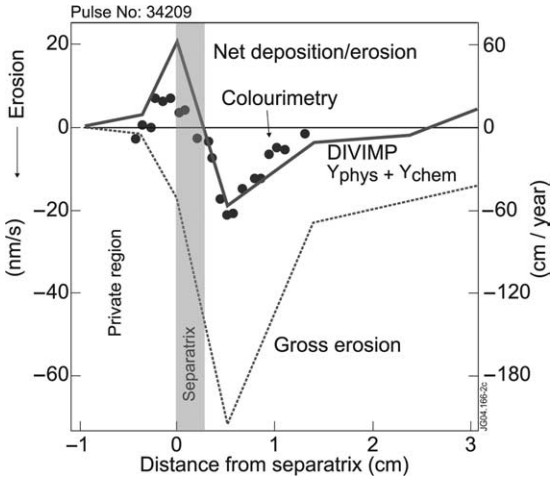

Fig. 2. Erosion/re-deposition pattern measured on the outer divertor target of the JET MkI divertor by colourimetry and DIVIMP code predictions [7]. The right hand axis gives an extrapolation to continuous operation.

mode plasmas in JET by the technique of colorimetry. Material is removed from near the strike point and deposited in the private region as predicted by the DIVIMP Monte-Carlo impurity transport code [7]. The net erosion in this example has a peak value of 20 nm/s which, due to low duty cycle, is of no practical consequence for JET but extrapolates to 60 cm per year if the plasma were run continuously as would be required in a fusion power plant. The calculated gross erosion rate, ignoring any replenishment of eroded surface areas by the re-deposited atoms, is 2.2 m per year. Erosion rates at the divertor target are expected to depend strongly on the plasma conditions. Fig. 3 shows that

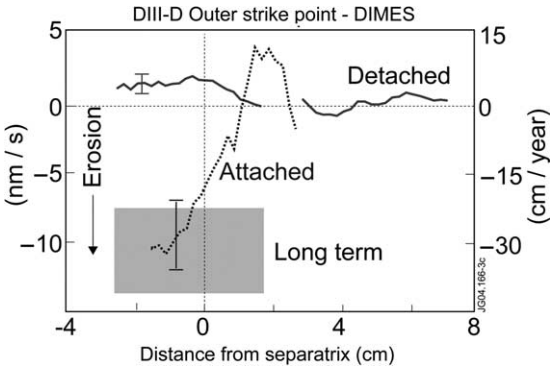

Fig. 3. Effect of divertor plasma conditions on the erosion/re-deposition measured with the DIMES sample probe in the outer divertor of DIII-D [8].

in DIII-D local measurements using a sample insertion probe (DIMES) switch from a classic erosion/re-deposition pattern, albeit not balanced, to one of net deposition which must come from a source outside the divertor [8].

2. Sputtering yields

Erosion of materials by physical sputtering is the most fundamental of plasma–surface interactions in tokamaks [9]. The surface binding energy for atoms in fusion relevant materials lies in the range 3–8 eV, so that provided an impacting ion or neutral is able to impart this much energy to a surface atom there is a finite probability of ejecting an atom from the surface. This probability is the physical sputtering yield which depends most strongly on the mass ratio between the impinging ions and target atoms since this determines the efficiency with which energy can be transferred to surface atoms, Fig. 4. There is a threshold energy for incident particles below which physical sputtering is impossible and this threshold rises with target mass and decreases with incident ion mass ($D \rightarrow C$ $E_{th} = 35$ eV, $D \rightarrow W$ $E_{th} = 220$ eV, $He \rightarrow W$ $E_{th} = 110$ eV).

The average ion impact energy, E_i, on a surface has contributions from ion acceleration in the sheath as well as the ion thermal energy, $E_i \approx 3ZT_e + 2T_i$ where Z is the charge state of the impinging ion. Fusion power plant divertor concepts involving solid targets rely on using the highest mass refractory metal, tungsten, in combination with a cold high recycling or detached divertor plasma. Because of their higher mass the presence of impurities is expected to strongly influence high Z erosion and impurity radiation is a key ingredient in keeping target power tolerable – current ITER solutions require ≈75% radiation [11] and higher values will be required in a power plant.

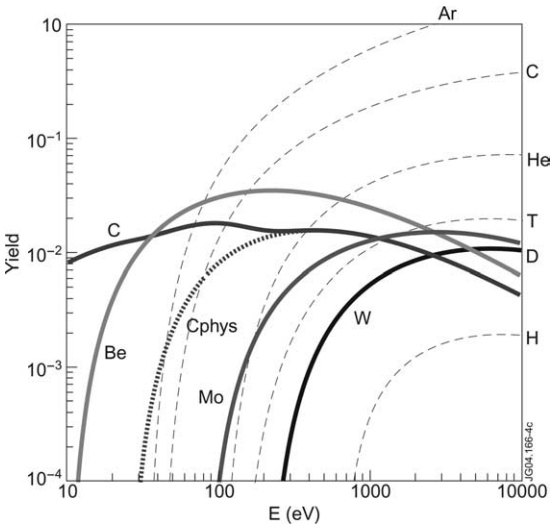

Fig. 4. Sputtering yield curves for various fusion relevant materials for bombardment by deuterium. In the case of tungsten physical sputtering yields for a range incident ion mass are plotted [44].

2.1. Chemical erosion of carbon materials

When JET was operated in helium at sufficiently high density, it was found that, as expected, the spectroscopic emission from C^{2+} ions (CIII) in the divertor falls to a very low level consistent with the physical sputtering threshold for carbon [10]. In deuterium however, the CIII signals remain high at all densities and this is attributed to chemical sputtering which clamps the yield at a high value right down to very low ion energies, Fig. 4.

Whilst important for current machines, chemical erosion is not considered a relevant issue for fusion power plants since the severe degradation of physical and mechanical properties of carbon based materials under high fluence neutron irradiation appears to rule them out for use in power plant plasma facing components [46]. In ITER, however, carbon fibre composite (CFC) tiles are to be used at the strike points (at least in the initial phase of ITER operation) which in addition to excellent mechanical and thermal properties is expected to be more resilient to power transients due the lack of a liquid phase, see Section 5. Because of its potential for tying up large quantities of tritium in hydrocarbon layers that makes the understanding of chemical erosion still a major area of study for ITER [6].

Under the very high particle flux density conditions predicted for the ITER divertor ($10^{24}\,m^{-2}\,s^{-1}$ [11]), some experimental data has suggested that chemical erosion yields may be suppressed. However, the data from different experiments have appeared contradictory until a recent initiative to regularise the data using common yield definitions and a selection of similar ion energies [12]. This process puts the experimental basis for flux dependence on a firmer footing and, combined with the dependence of chemical yield on surface temperature, a significant reduction in chemical erosion rate is predicted for ITER by the ERO code [13] bringing the net erosion rate down by more than an order of magnitude compared with the standard assumption of constant 1% chemical yield.

There are other effects that may also help reduce carbon chemical erosion yields in ITER. In DIII-D, a reduction in the ratio of CD molecular band emission to D_α radiation over a time-scale of years has been interpreted as a reduction in chemical erosion with fluence [8]. What might cause this effect and why it has not been observed in all other machines with carbon divertors is not yet known. Migration of beryllium from the main wall material in ITER to the divertor is also expected to suppress chemical erosion of carbon plasma facing surfaces as has been observed in the PISCES linear machine [14]. However, the stability of Be-C films in the presence of large thermal transient due to ELMs and disruptions is a critical issue.

3. Long term material migration – global and macroscopic

The simple picture of material migration outlined in Section 1 has two implicit assumptions: The first is that each leg of the divertor is a self-contained system with no interplay with other sources or sinks of impurities. The second is that re-deposited atoms behave identically to the original material.

In Fig. 5, the long term erosion/deposition measured directly by micrometer is shown for the JET MkIIGB divertor for the operational period 1999–2001 [15]. This data shows that in the outer divertor the erosion/deposition is more or less neutral with the exception of a narrow band of deposition in the outer pump duct. The inner divertor on the hand shows strong net deposition over the whole of the target with a large deposit of soft compressible material in the inner pump duct. Flakes formed by peeling of thick hydrocarbon films are also found in the shadowed areas of the inner divertor corner with D:C ratios up to 0.7. Analysis of similar flakes from the JET tritium campaign showed that they are responsible for the majority of the long term tritium retention.

These results demonstrate that most of the carbon deposition found in the divertor must have originated from erosion of the main chamber wall with preferential deposition in the inner divertor. It is also clear that the surface layers cannot be treated simply as extension of the substrate since in JET carbon migrates into the shadowed corner of the inner divertor at a rate which is at least an order of magnitude greater than simple models predict.

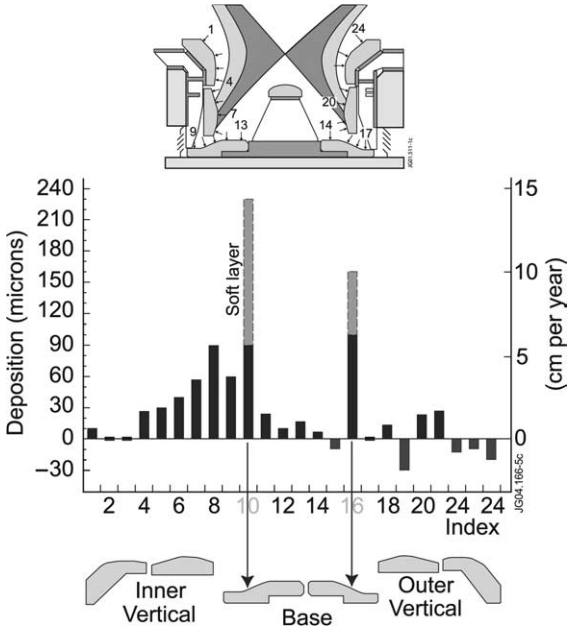

Fig. 5. Erosion/deposition measured by micrometer gauge in the JET divertor following the 1999–2001 MkIIGB divertor phase of JET [15].

Details vary between tokamaks but most devices see similar evidence for net deposition of main wall material in the divertor with much stronger deposition at the inner target.

Migration of significant amounts of carbon into remote areas is also commonly, although not universally, reported in both limiter and divertor machines.

3.1. Carbon migration to remote areas

Following work on laboratory plasmas [16] the idea emerged that C_2H_x hydrocarbon molecules or radicals might be released by thermal decomposition of soft hydrocarbon films formed on hot surfaces (above 500 K) in the inner divertor. Soft films are formed when the ion impact energy is less than 30 eV whilst hard films, which show a much higher temperature threshold for release of hydrocarbons, form at ion energies above 50 eV. The view was put forward that the large amounts of carbon found in remote areas in JET during the tritium campaign (DTE1 [17]) might be a consequence of the formation of soft films and consequent decomposition (JET tile temperature ~500 °K) into low sticking coefficient fragments which might attach themselves preferentially to the water cooled louvers at the end of the pump ducts, Fig. 5. This interpretation generated a concern that substantial quantities of low sticking probability hydrocarbon molecules containing tritium might be deposited in remote areas of ITER such as the pump ducts where they would be difficult remove [16].

Measurements of sticking probability [1] in JET [18] using cavity probes show that 99.8% of molecules have a sticking coefficient of 0.92 whilst 0.2% have a sticking coefficient of <0.01. This implies that the migration to remote areas in JET is related mainly to the decomposition of layers in plasma facing areas rather than a high proportion of low sticking coefficient molecules. Diagnosis of the pump ducts in ASDEX-Upgrade has revealed rather low deposition rates [19] which suggests a similar interpretation. The combination of high sticking yet high re-erosion probability is also nicely demonstrated by TEXTOR data [43].

3.2. SOL flow and divertor asymmetries

The large asymmetry in carbon deposition between the inner and outer divertors is commonly believed to be a consequence of the flow pattern which has been observed in the scrape-layer with Mach probes. This flow pattern is strongly dependent on the sign of the magnetic field which suggests that classical drifts play an important role. In Fig. 6, parallel Mach number measurements are compared for similar L-mode plasmas in JT60-U [20] and JET [21]. Mach probe data from C-Mod shows a qualitatively very similar overall flow pattern to JET and JT60-U with large flows being measured towards the inner divertor at the inner mid-plane with the ion grad B drift both towards and away from the divertor [45]. These measurements show that the stagnation point in the flow is between the outer mid-plane and the outer strike-point in the normal field direction (grad B drift down) but moves to the top of the machine with reversed field. Recent observations of IR surface anomalies in JET have shown that prolonged operation in reversed field leads to the development of surface layers across the outer target which are similar to those at the inner target and disappear over time when the normal field direction is restored [22].

Classical drifts as implemented in 2D fluid codes can reproduce the behaviour of the parallel Mach number measurements qualitatively [20,21] but are too small in key areas and so other processes are also being considered such as ballooning transport [23]. It should also be noted that the impurity flow is only strongly coupled to the flow of the hydrogenic ions in the outer SOL where the collisionality is high enough. Closer to the separatrix the ion temperature gradient force becomes dominant [3]. Interpretation of real SOL flow data with 2D codes is still in its infancy and is a complex problem. In JT60-U for example, $E_r \times B$ poloidal drifts are

[1] Strictly speaking cavity probes measure surface loss probability [16] which does not account for differences in structure of molecules incident on and released from surfaces.

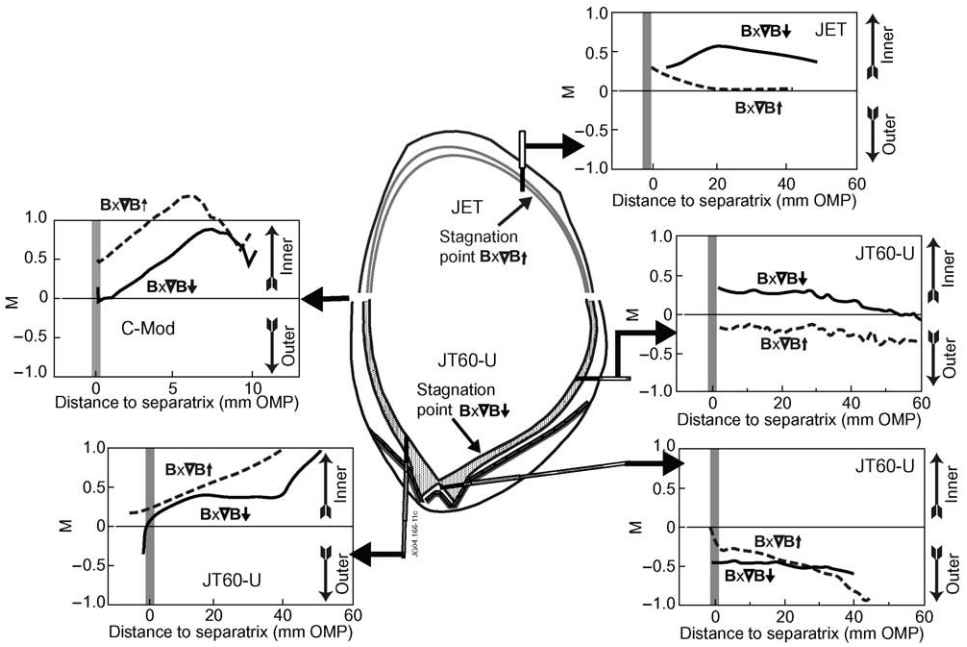

Fig. 6. Composite comparing Mach number profiles measured by probes in JT60-U [20], JET [21] and C-Mod [45] (inner wall probe only and combining upper and lower target data). The approximate stagnation points for forward and reversed B cases are indicated.

measured to be important and the UEDGE code predicts a strong flow from outer to inner target via the private region which might provide a path for impurities to reach the inner divertor [20].

Although SOL flows have been the main focus of argument regarding the in/out asymmetries in material deposition, it is also probable that the associated asymmetry in divertor parameters plays a significant role [23,24]. Although chemical sputtering complicates the picture, it is evident that for most materials the strong energy dependence of the sputtering yield means that temperature asymmetries alone could shift the equilibrium from net erosion in one divertor to net deposition in the other.

More specific experimental data may be able to resolve these questions. In JET for example, $^{13}CH_4$ was injected at the top of the machine (2.8 g ^{13}C) in 12 identical ohmic pulses on the last day of campaign and surface analysis showed 100 times more ^{13}C in the inner divertor and no evidence for migration to remote areas [25]. These results suggest that SOL drifts rather than re-erosion at the outer target is the principal cause of the asymmetry. Quartz micro-balance data suggests that the absence of ^{13}C inside the inner pump duct may be the result of operation in a single plasma configuration (Section 3.1 – line of sight deposition), coupled with low power plasmas and an absence of ELMs [42]. Very similar results to those in JET have been obtained from $^{13}CH_4$ injection at the top of DIII-D [49] into L-mode plasmas but with the benefit of a toroidally symmetric source. Analysis of the plume associated with this methane puff suggests Mach numbers around 0.4 towards the inner divertor [50,51].

4. Migration accounting

4.1. Low *Z* walls

In JET, two totally independent means have been used to evaluate the total main wall source of carbon in a wide range of specific shots [3]. The first involves using the EDGE2D/NIMBUS coupled multi-fluid and Monte-Carlo code to provide a scaling between the spectroscopic intensity on specific lines of sight and the total main wall source. Potential errors in this case are most likely due to differences in poloidal distribution of sources and plasma parameters between model and experiment. The second technique involves prediction of the main wall source from the core Z_{eff} coupled with experimentally determined screening factors for CD_4 puffed at different poloidal locations. The two approaches are in good agreement although the Z_{eff} method produces intrinsically higher scatter. Divertor and wall sources computed by the spectroscopic technique are plotted in Fig. 7 [3]. Main wall erosion reaches 1000 kg/year calculated for continuous operation of high performance pulses and ten times this amount is seen in the divertor due to recycling of carbon prior to loss to remote areas.

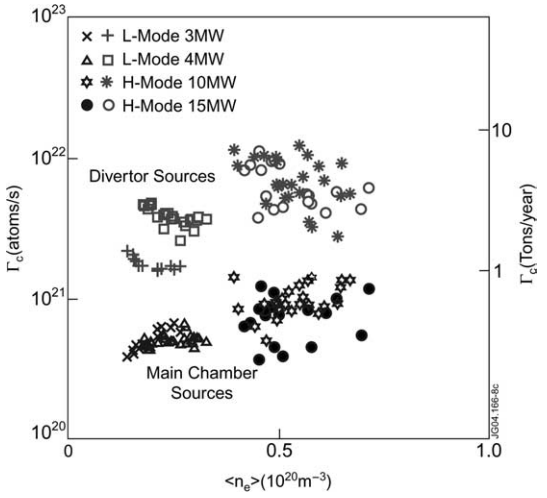

Fig. 7. Total divertor and wall carbon sources evaluated from CIII spectroscopy [3]. Right hand axis shows an extrapolation of the sources for continuous operation.

Consistency of spectroscopic data for the main wall sources with data from surface analysis of divertor tiles can be checked by integration over whole campaigns. This should show a main wall source equal to or greater than the measured divertor deposition (some impurities may return to the main wall). Initial results showed net divertor deposition at least 3 times higher than total wall source which is impossible [26]. Application of more quantitative surface techniques has however now brought the data for the 1999–2001 campaign (16 h of divertor plasma) into line [27], the accounting is now as follows (extrapolations to continuous operation for a whole year are included for reference) – main wall sources: Be(BeII) = 20 g (wall coverage ≈20%), C(CIII) = 450 g, 480 g C (Z_{eff}). Divertor deposition: Be = 22 g(12 kg/year), C = 390 g(220 kg/year) – mainly inner divertor.

In ASDEX-Upgrade a similar accounting has been carried out for the period 2002/3 (1.4 h of plasma) when the inner wall was entirely coated with tungsten. Surprisingly, the inner wall carbon source determined spectroscopically did not decrease substantially and the carbon is believed to recycle there. This is a cautionary tale showing that spectroscopic data have to be interpreted with great care since, without the tungsten coating, we would not know that the inner wall was not a net carbon source. The story of the carbon balance in ASDEX-Upgrade divertor is also rather complicated with new evidence for substantial erosion in the outer divertor possibly exceeding the net main wall source by an order of magnitude [28]. Total inner divertor deposition however extrapolates to (215 kg/year) which is very close to the JET value.

4.2. High Z walls

The general conclusions of the tungsten wall experiment so far in ASDEX-Upgrade are that the inner wall erosion rate extrapolates to 45 kg/year for continuous operation but that at least 2/3 of this is associated with the limiter phase. Of this amount, a deposition rate of only 9 kg/year has been measured back at the inner wall whilst 2.5 kg/year is found at the inner divertor target and 1.5 kg/year at the outer divertor target [29]. Most of the erosion is thought to be due to sputtering by impurities. So whilst ASDEX-Upgrade has experienced no insuperable operational problems when operating with a tungsten inner wall it is hard to draw any real conclusions about the erosion rate in a full tungsten machine due to the continued dominance of carbon. Recent results from a few tungsten tiles placed at the outer limiter suggest that due to fast particles erosion rates may be and order of magnitude higher here [47].

C-Mod is the only divertor machine currently operational with a full high Z wall, in this case molybdenum. Erosion/re-deposition rates have been measured in C-Mod by surface analysis [30]. Since C-Mod operates mainly at high density with low divertor electron and ion temperatures, then as expected from the high sputtering threshold for molybdenum (Fig. 4), the peak erosion rate in the outer divertor is low (0.14 nm/s or 0.45 cm/year). This is about a factor 100 lower than the peak erosion rate measured in specific attached discharges in DIII-D and JET, Figs. 2 and 3. However, such comparisons are a little questionable given that DIII-D also reports low erosion rates in detached discharges and JET shows little net erosion at the outer target (Section 1). Despite this caveat, there is no doubt that, under the right plasma conditions, high Z can deliver low erosion rates.

4.3. Steady state erosion of the main walls

The erosion rate of the main chamber walls depends simply on the fluxes and energy distributions of neutral atoms and ions arriving there. Recent comparison of current divertor tokamaks has shown that the total fluxes of neutral atoms, integrated over the whole main chamber wall, are very similar in absolute magnitude and thus roughly independent of size, Fig. 8 [31]. It is interesting to note that current ITER predictions [32] are also consistent with this finding, Fig. 8. The greatest uncertainty in these extrapolations now comes from the question of how the ion component of the wall flux scales with machine size due to enhanced turbulent transport which has been observed in the far scrape-off layer of some tokamaks [31]. The extent to which fuelling with pellets might reduce edge neutral pressure compared with gas puffing is also an issue.

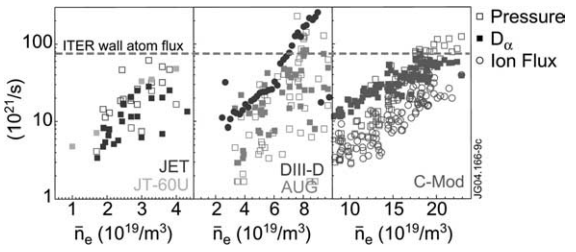

Fig. 8. Total main chamber ion and neutral fluxes for a range of tokamaks [31]. The predicted value for ITER is also shown [32,48].

5. Erosion by transients

5.1. ELMs in ITER

In ITER, although predictions have become more sophisticated and less pessimistic, it is still thought that even the smallest type I ELMs may be marginal with respect to ablation of the divertor target when factors such as statistical variability and asymmetries are taken into account [33,34]. Ablation of the CFC material is a concern for ITER because calculations suggest that the target lifetime due to erosion decreases rapidly once a certain surface energy density is exceeded (1–2 MJ/m^2) [33]. Tungsten performs better than CFC in this analysis although the actual gain of up to a factor 2 is dependent on what fraction of the thin molten surface layer is assumed to be lost during the ELM event due to the effect of electromagnetic forces.

The total thermal stored energy in high performance plasmas increases strongly with machine size, W_{th} (MJ) $\approx$ DIII-D 1, JET 10, ITER 350, DEMO 1500 (note that there is no official description of DEMO but it will be assumed similar to ITER-FDR [35]). Due to the rather weak scaling of ELM duration and divertor wetted area with machines size, the approximate ELM energy threshold above which ablation of a carbon divertor is expected to significantly reduce target lifetime scales roughly as: $\Delta W_{ELM}/W_{th} \approx$ DIII-D 100%, JET 15%, ITER 2%, DEMO <1%. This means that the largest ELMs in JET can be used to study ablation by ELMs whilst in ITER even small type I ELMs may exceed the threshold.

5.2. ELMs in power plants – ELM buffering

The effect of ELMs on wall lifetime in fusion power plants that may follow on from ITER has not yet been considered [32]. The relatively low duty cycle in ITER means that ablation by ELMs is the primary concern [33]. In a power plant however, the effect of ELMs on the erosion of high Z walls and targets by the energetic ions produced by ELMs still needs to be considered.

At the target, the question is to what extent an ELM pulse can be cooled such that the impact energy of ions within the divertor does not rise significantly above the sputtering threshold for tungsten. The most comprehensive analysis of the effect of radiation on the dissipation of ELM energy has been carried out at JET [36]. Both in the experiment and in time-dependent simulation with EDGE2D/NIMBUS, the results show that only very small ELMs can be dissipated. Strongly detached nitrogen seeded shots in JET are calculated to have ion impact energies which are below the threshold for sputtering of tungsten by tritons, Fig. 9. However, even a small ELM corresponding to only 0.15% of total thermal stored energy drives the calculated impact energy over the sputtering threshold. Similar ITER simulations using the B2/EIRENE code found significant dissipation of ELM energy for W_{ELM}/W_{th} <0.3% [37].

In additional to enhancing the erosion of high Z divertor targets there is also now reason to believe that ELMs in large tokamaks will enhance the erosion of a high Z main chamber for similar reasons. Recent measurements of the radial propagation of ELMs on JET [38] have been fitted to a model which considers the energy balance of a plasmoid ejected from the pedestal region. The results suggest that while the electrons in the ELM plasmoid cool rapidly, the loss of ion energy is much slower and the calculated ion impact energy at the limiter radius, is expected to rise strongly with machine size. The sputtering yield at the limiter for tungsten due to fuel ions ejected by an ELM is predicted to reach 1% in ITER conditions [38]. Depending on the total ion flux due to ELMs in the far SOL, these events

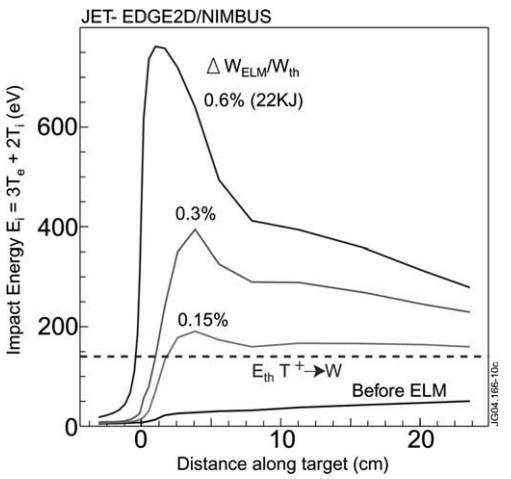

Fig. 9. EDGE2D/NIMBUS simulations of the ion impact energy at the outer divertor target for a completely detached nitrogen seeded H-mode. The effect of ELMs of different sizes is shown [36].

could contribute significantly to the erosion of high Z main walls.

5.3. Disruptions

The energy density, averaged over the whole of the plasma surface area, also scales strongly with machine size, W_{th}/A_{plasma} (MJ/m^{-2}) ≈ DIII-D 0.02, JET 0.05, ITER 0.5, DEMO 1.2. The implication of this is that, unless disruptions are almost perfectly mitigated by massive puffs of noble gases in ITER or DEMO, a melt layer could be created over a significant fraction of the main wall [39]. However, it should be noted that the consequences are very dependent on the extent and thickness of any melt layer and how much of it migrates to other areas – metal droplets of high Z materials (but not low Z [40]) may also trigger disruptions. In the diverted phase of ITER, the average power load on the main wall is less than 0.2 MW/m^2 whilst in DEMO it is around 0.5 MW/m^2 neither of which is very demanding so that some surface melting can probably be tolerated [40]. The situation in the divertor is different because it has to operate at the maximum possible power density and so surface damage in this area will be less acceptable – hence the importance of disruption mitigation [39].

6. Extrapolations to future power plant scale tokamaks

Divertor target erosion rates are very difficult to predict in conventional fusion power plant concepts with solid high Z targets because the net erosion or deposition is strongly dependent on plasma parameters. The fraction of ions arriving above the sputtering threshold is crucial, as is the efficiency of the prompt local re-deposition. ELMs have not really been considered in this context but we can see from the analysis in Section 5 that ELMs in power plant systems will have to be extremely small – much smaller than will be allowable in ITER which still has a relatively low duty cycle. The ideal would in fact be a quiescent ELM free high density steady state edge plasma.

Calculations of the minimum erosion rate for the main wall are somewhat more robust since there has to be a hot plasma in the main chamber and the rate of leakage of neutrals into the main chamber from the divertor is calculable using Monte-Carlo codes. Comparison of charge exchange energy spectra at the outer mid-plane calculated by B2/EIRENE for ASDEX-Upgrade and ITER show rather little dependence on machine size [48]. The contribution made by ion flux to the walls and limiters due to transport in the peripheral SOL is the main source of uncertainty. In a recent study of different wall materials, the standard ITER B2/EIRENE reference plasma [11] was used and the wall materials changed [32]. This analysis compared Be, C, Fe, Cu, Mo and W walls with the conclusion that in all cases the erosion rate was 1–2 tons per year of continuous operation (30 g per ITER pulse for a beryllium wall). The time taken to erode 5 mm of main wall tungsten armour is predicted to be about 20 years [32] but only 2 years for beryllium due to the difference in density but it should be remembered that no account has been taken of the effect of ELMs. It is interesting to note that we would also predict carbon erosion of around 1 ton per year for continuous ITER operation if we combine the JET results of Fig. 7 with the wall neutral flux scaling of Fig. 8.

In fusion power plants, and possibly also in ITER, all deposited material will behave as if it has zero sticking in the long term because surface layers will reach a critical thickness where internal stresses compounded by thermal transient (ELMs) will cause them flake off. Systems will be needed to extract [41] and process this debris which will other pose problems due to safety limits imposed by activated dust and retained tritium.

7. Conclusions

Material migration does not present any significant operational issues for current tokamaks but in this paper results are reviewed which show that it will become increasingly important as we move to ITER and then onwards to a demonstration fusion power plant. Optimisation of both the plasma and plasma-facing materials to minimise migration is essential in both cases. Management of the tritium retention in migrated material will also be critical. The complexity of the problem means that predictions will remain uncertain and techniques to live within material limits difficult to develop without full wall material tests in current tokamaks, combined with components of relevant geometry.

Acknowledgments

I would particularly like to thank W. Fundamenski, Y. Chen, J.P. Coad, D. Coster, K. Krieger, Y. Likonen, A. Loarte, A. Kallenbach, A. Kukushkin, M. Mayer, V. Philipps and J. Strachan for their specific contributions. This work has been conducted under the European Fusion Development Agreement and is partly funded by Euratom and the United Kingdom Engineering and Physical Sciences Research Council.

References

[1] C.S. Pitcher, P.C. Stangeby, Plasma Phys. Control. Fus. 39 (6) (1997) 779.
[2] P. Stangeby, The plasma boundary of magnetic fusion devices, Book ISBN 0 07503 0559 2, Chapters 5 and 6.

[3] J.D. Strachan et al., Nucl. Fus. 43 (2003) 922.
[4] A. Kirschner et al., J. Nucl. Mater. 313–316 (2003) 444.
[5] J. Brooks et al., J. Nucl. Mater. 266–269 (1999) 58.
[6] G. Federici et al., Nucl. Fus. 41 (12) (2001) 1967.
[7] H.Y. Guo et al., J. Nucl. Mater. 241–243 (1997) 935.
[8] D. Whyte et al., J. Nucl. Mater. 290–293 (2001) 356.
[9] R.A. Langley et al., Nucl. Fus., Special Issue 1984, IAEA, Vienna (1984).
[10] R.A. Pitts et al., J. Nucl. Mater. 313–316 (2003) 777.
[11] A. Kukushkin et al., Nucl. Fus. 42 (2) (2002) 187.
[12] J. Roth et al., Nucl. Fus. 44 (2004) L21.
[13] J. Roth, A. Kirschner et al., these Proceedings. doi:10.1016/j.jnucmat.2004.10.115.
[14] R. Doerner, in: 10th Carbon Workshop Julich, 2003.
[15] P. Coad, J. Nucl. Mater. 313–316 (2003) 419.
[16] A. von Keudell et al., Nucl. Fus. 39 (10) (1999) 1451.
[17] P. Coad, J. Nucl. Mater. 290–293 (2001) 224.
[18] M. Mayer et al., in: Proceedings of the 30th EPS Conf. (St. Petersburg, 2003) Europhysics Conference Abstracts Vol. 27A, O-2.6A.
[19] M. Mayer et al., J. Nucl. Mater. 313–316 (2003) 429.
[20] N. Asakura et al., Nucl. Fus. 44 (4) (2004) 503.
[21] S.K. Erents et al., Plasma Phys. Control. Fus. 46 (11) (2004) 1757.
[22] P.Andrew et al., these Proceedings. doi:10.1016/j.jnucmat.2004.10.145.
[23] R.A. Pitts et al., these Proceedings. doi:10.1016/j.jnucmat.2004.10.111.
[24] W. Fundamenski, these Proceedings. doi:10.1016/j. jnucmat.2004.08.030.
[25] J. Likonen et al., Fus. Eng. Des. 66–68 (2003) 219.
[26] G.F. Matthews et al., in: 30th EPS Conf. (St. Petersburg, 2003), Europhysics Conference Abstracts Vol. 27A, P-3.198.
[27] J. Likonen, these Proceedings. doi:10.1016/j.jnucmat.2004.10.151.
[28] M. Mayer et al., these Proceedings. doi:10.1016/j.jnucmat.2004.10.046.
[29] K. Krieger et al., J. Nucl. Mater. 313–316 (2003) 327.
[30] W.R. Wampler et al., J. Nucl. Mater. 266–269 (1999) 217.
[31] B. Lipschultz et al., in: 18th IAEA Fusion Energy Conf. (Sorrento 2000) paper EX5/6.
[32] R. Behrisch et al., J. Nucl. Mater. 313–316 (2003) 388.
[33] G. Federici et al., Plasma Phys. Control. Fus. 45 (9) (2003) 1523.
[34] A. Loarte et al., Plasma Phys. Control. Fus. 45 (9) (2003) 1549.
[35] ITER Physics Expert Group, Nucl. Fus. 39 (1999) 2137.
[36] J. Rapp et al., Nucl. Fus. 44 (2) (2004) 312.
[37] A. Loarte et al., in: 18th IAEA Fusion Energy Conference (Sorrento 2000) paper ITERP/11(R).
[38] W. Fundamenski et al., Plasma Phys. Control. Fus. 46 (2004) 233.
[39] D. Whyte et al., J. Nucl. Mater. 313–316 (2003) 1239.
[40] A. Loarte, these Proceedings. doi:10.1016/j.jnucmat.2004.09.038.
[41] M. Wykes et al., Fus. Eng. Des. 56–57 (2001) 403.
[42] G. Esser et al., these Proceedings. doi:10.1016/j.jnucmat.2004.10.112.
[43] J. von Seggern, A. Kirschner, V. Philipps, et al., Phys. Scr. T 111 (2004) 118.
[44] W. Eckstein et al., IPP Garching report number IPP 9/82 (1993).
[45] B. LaBombard, J.E. Rice, A.E. Hubbard, et al., Nucl. Fus. 44 (2004) 1047.
[46] T. Burchell, Phys. Scr. T 64 (1996) 17.
[47] R. Dux et al., these Proceedings. doi:10.1016/j.jnucmat.2004.10.105.
[48] A. Kukushkin, D. Coster, Y. Chen, private communication, June 2004.
[49] S. Allen et al., these Proceedings. doi:10.1016/j.jnucmat.2004.09.066.
[50] A. McLean et al., these Proceedings. doi:10.1016/j.jnucmat.2004.10.130.
[51] D. Elder et al., these Proceedings. doi:10.1016/j.jnucmat.2004.10.138.